Electronic Supplementary Material (ESI) for Analyst.

Supporting Information

A dual-emitting immunosensor based on manganese dioxide nano flowers and zinc sulfide quantum dots with enhanced electrochemiluminescence performance for the ultrasensitive detection of procalcitonin

Na Wang, Juan Yang, Zhi Luo, Dongmiao Qin, Yusheng Wu and Biyang Deng*

State Key Laboratory for Chemistry and Molecular Engineering of Medicinal Resources, School of Chemistry and Pharmaceutical Sciences, Guangxi Normal University, Guilin 541004, China

*Corresponding Author:

Email: dengby16@163.com

Table of Contents

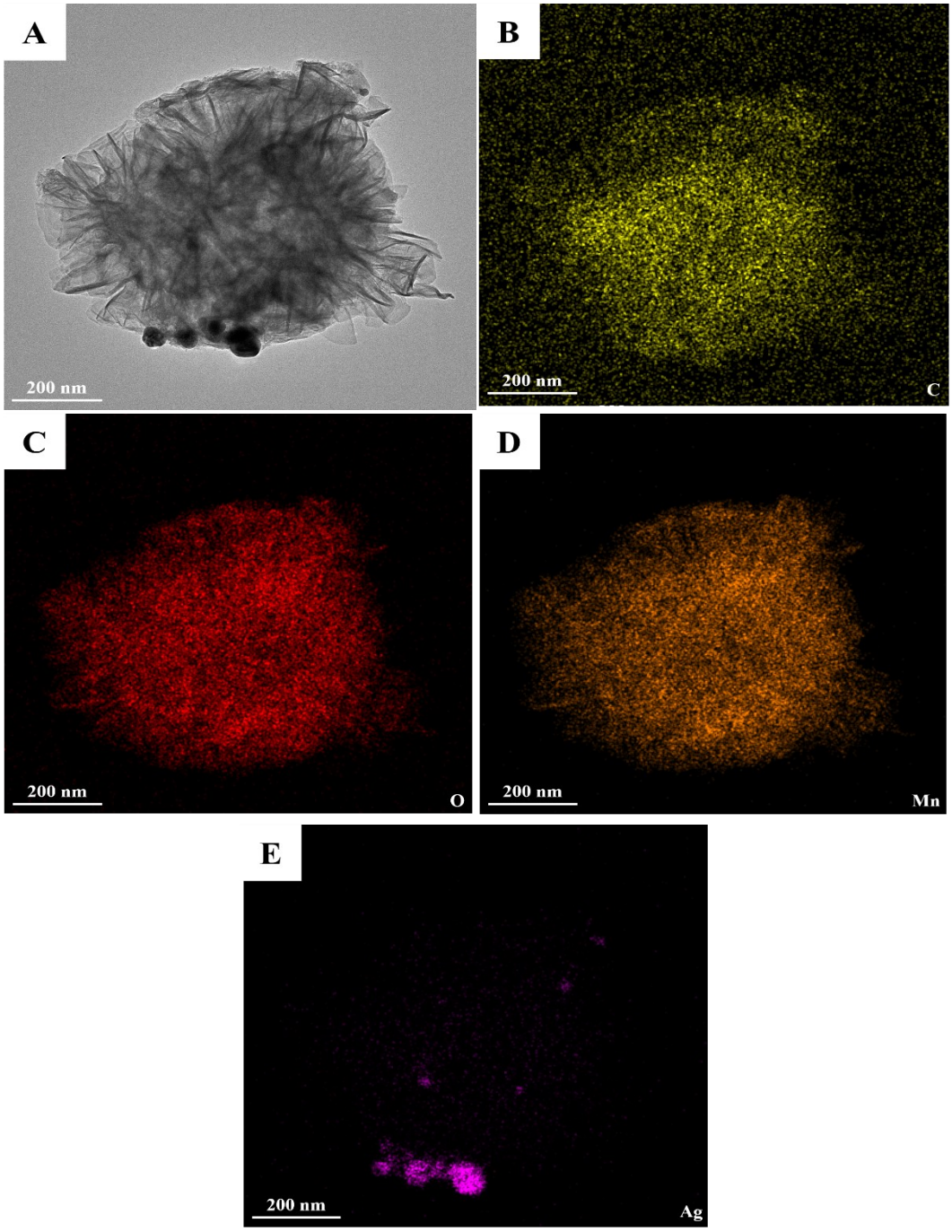

Fig. S1 (A) TEM image of the MnO_2NFs/PDDA-Ag; TEM-EDS elemental mapping of (B) C, (C) O, (D) Mn, and (E) Ag elements of the MnO_2NFs/PDDA-Ag.

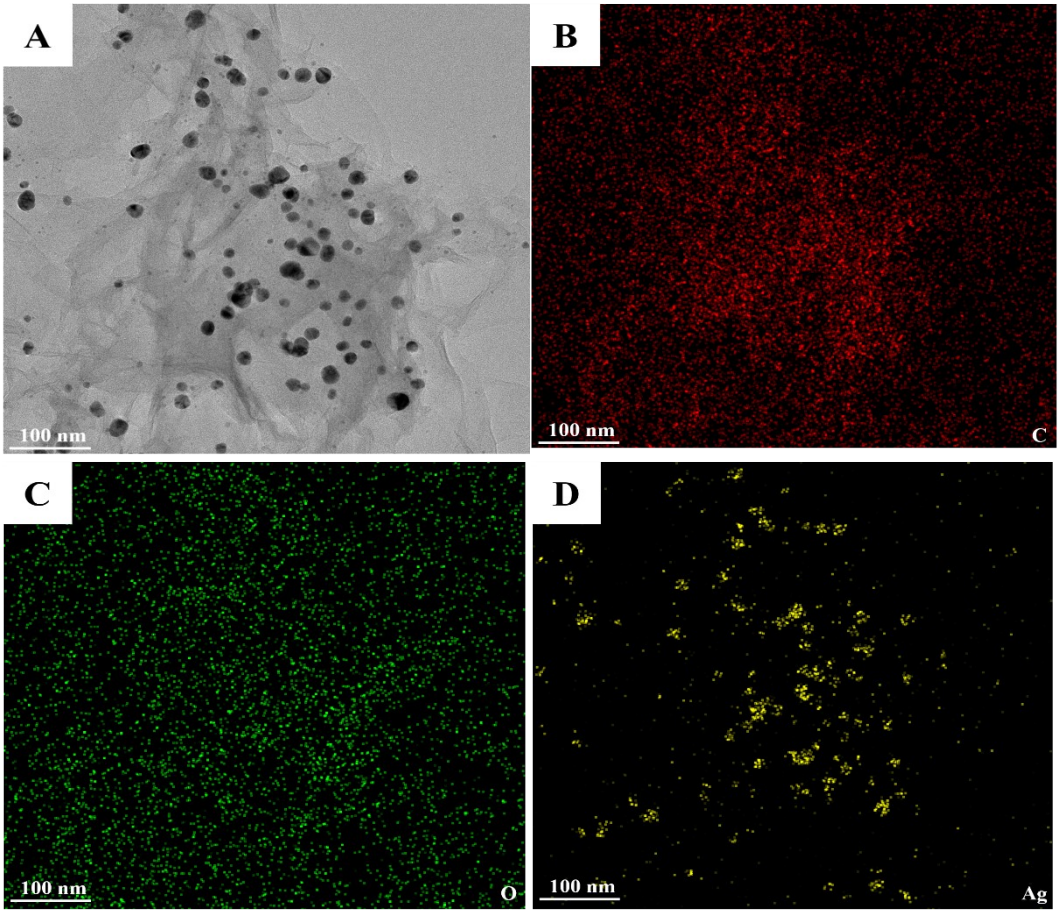

Fig. **S2** (A) TEM image of the rGO@Ag; TEM-EDS elemental mapping of (B) C, (C) O, and (D) Ag elements of the rGO@Ag.

UV-vis spectra and FT-IR spectrum of the prepared materials

The AgNPs and rGO@Ag were characterized by UV–vis spectroscopy (Fig. S3A). The UV-vis spectrum of the AgNPs (curve a, black) featured a distinct absorption peak at 410 nm, while the UV-vis spectrum of the rGO@Ag composite (curve b, red) featured characteristic absorption peaks at 260 nm and 410 nm. The absorption band at 260 nm was attributed to the π-π* transitions of aromatic C=C bonds,[1] while the presence of the absorption band at 410 nm in the spectrum of the rGO@Ag composite indicated that the AgNPs were successfully assembled on the graphene sheets.

Fig. S3B shows the FT-IR spectrum of the amine-functionalized ZnSQDs. The absorption bands at 3430 $cm^{-1}$and 1633 cm^{-1} corresponded to the -NH stretching vibrations and bending vibrations, respectively, while the band at 1116 cm^{-1} corresponded to the -CN stretching vibrations. These result demonstrated that the surface of ZnSQDs contained -NH_2 groups, as expected.

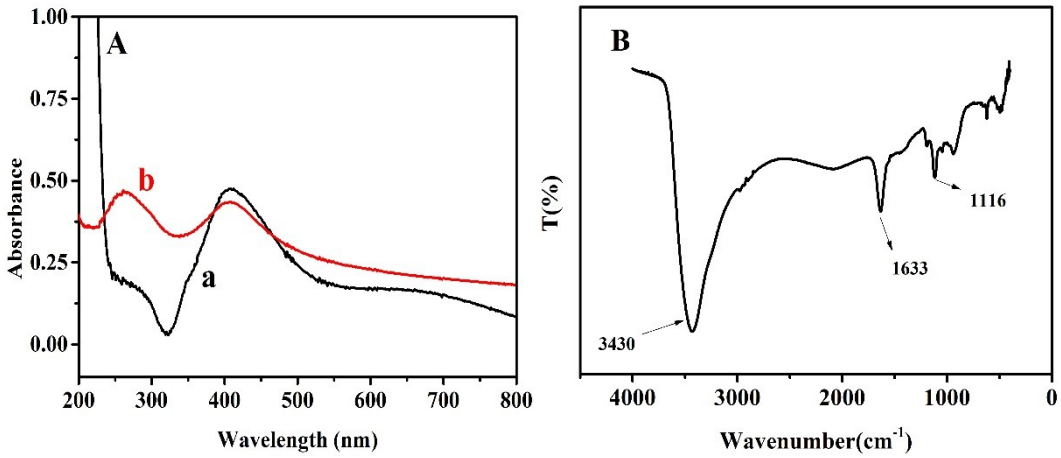

Fig. S3 (A) UV–vis absorption spectra of the AgNPs (a) and rGO@Ag (b); (B) FT-IR spectrum of the ZnSQDs.

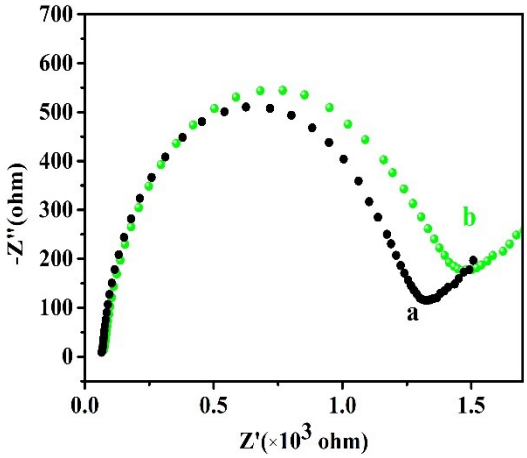

Fig. **S4** EIS spectra of the modified electrodes: GCE/rGO@Ag (a), GCE/rGO (b).

Optimization of the experimental conditions

The concentration of $K_2S_2O_8$, the pH of PBS, the volume of 10 μg/mL Ab1, the incubation time of the modified GCE in the PCT solution, and the scanning rate of potential were optimized to achieve the best analytical performance for the detection of PCT by the modified GCEs. During the preliminary optimization experiments, the PCT concentration was held constant at 0.1 ng/mL. As shown in Fig. S5A, when the concentration of $K_2S_2O_8$ increased from 0.02 mol/L to 0.1 mol/L, the ECL intensity increased from 1067 a.u. to 5992 a.u. because more $SO_4^{\bullet-}$ was produced as the concentration of $K_2S_2O_8$ increased. However, the ECL intensity decreases when the concentration of $K_2S_2O_8$ exceeds 0.1 M due to excessive $S_2O_8^{2-}$ hinder MnO_2NFs/PDDA-AgNPs aggregation on GCE surface, and reduce the generation of MnO_2NFs^- and $ZnSQDs^-$. Therefore, 0.1 mol/L $K_2S_2O_8$ was chosen as the optimal concentration.

As shown in Fig. S5B, the ECL intensity of prepared immunosensor was highest when the pH of the PBS was 7.4, likely because more acidic and more alkaline pH values deleteriously affected protein activity and the binding efficiency of PCT (antigen) to the antibody. Therefore, pH 7.4 was chosen as the optimal pH of PBS solution.

The amount of Ab1 loaded onto the modified GCE had a great influence on the ECL intensity. As shown in Fig. S5C, the ECL intensity increased when the volume of the Ab1 stock solution increased from 10 μL to 50 μL. However, when the volume of Ab1 exceeded 50 μL, the ECL intensity gradually decreased because the excess antibody hindered electron transport. Therefore, 50 μL of Ab1 was selected as the optimum volume of the Ab1 stock solution. In addition, the effect of the incubation time of the immunosensor in the PCT solution (0.1 ng/mL) on the ECL intensity was investigated.

As shown in Fig. S5D, the ECL intensity decreased as the incubation time increased from 1947 a.u. to 5945 a.u. and then became stable when the incubation time exceeded 60 min. This indicated that the binding of the surface of the modified GCE became saturated with the antigen after 45 min. Therefore, 45 minutes was selected as the optimum incubation time for the following experiments.

The effect of the scan rate on the ECL intensity was investigated. As shown in Fig. S5E, the ECL intensity gradually increased from 3334 a.u. to 17452 a.u. as the scanning rate increased from 0.05 to 0.2 V/s, which might have been due to the rapid accumulation of free radical species at higher scanning rates, leading to higher ECL intensities. However, when the scan rate exceeded 0.2 V/s, the ECL intensity decreased from 17452 a.u. to 7458 a.u., which might have been caused by the high scan rate that prevented the $K_2S_2O_8$ from diffusing to the electrode surface in time.[2]

The effect of the amount of MnO_2NFs/PDDA-Ag on the ECL intensity of ZnSQDs was investigated. As shown in Fig. S5F, the ECL intensity increased as the volume increased from 0.5 mL to 2 mL. Beyond 2 mL, ECL intensity stabilized as MnO_2NFs/PDDA-Ag reached saturation binding with ZnSQDs. Therefore, the optimal volume of MnO_2NFs/PDDA-Ag was 2 mL.

The influence of the amount of rGO@Ag on the ECL intensity was also investigated. As

shown in Fig. S5G, the ECL intensity increased as the volume increased from 0.25 mL to 1 mL. Above 1 mL, ECL intensity stabilized due to the saturation of rGO@Ag and Ab1. Therefore, 1 mL was chosen as the optimized volume of rGO@Ag.

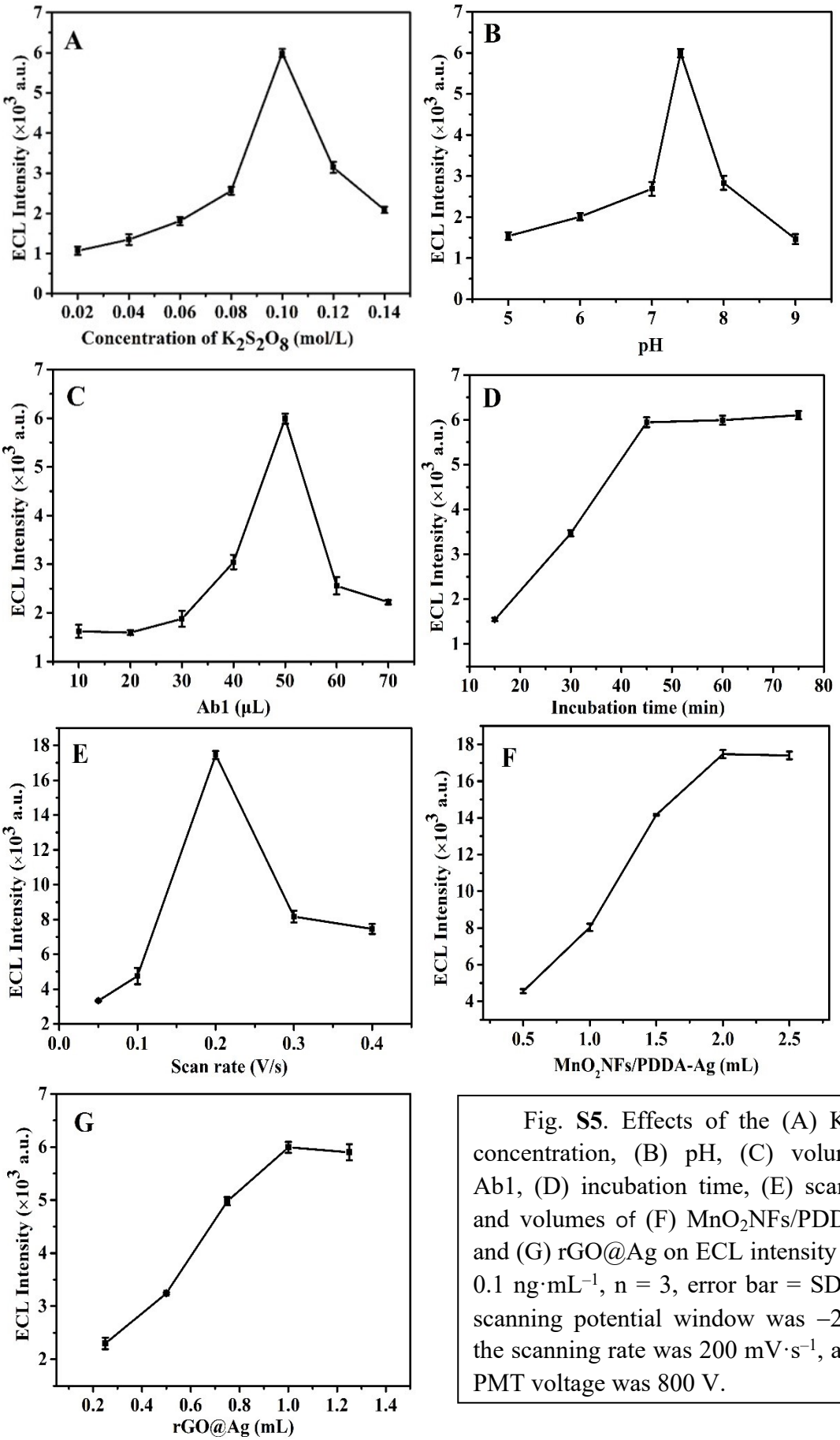

Fig. **S5**. Effects of the (A) $K_2S_2O_8$ concentration, (B) pH, (C) volume of Ab1, (D) incubation time, (E) scan rate, and volumes of (F) MnO_2NFs/PDDA-Ag and (G) rGO@Ag on ECL intensity (PCT: 0.1 ng·mL^{-1}, n = 3, error bar = SD). The scanning potential window was –2–0 V, the scanning rate was 200 mV·s^{-1}, and the PMT voltage was 800 V.

Table S1. Comparison between the ECL immunosensor reported herein and previously reported PCT detection methods

Method/Material	Linear range (ng/mL)	LOD (pg/mL)	Reference
ECL/RuSiNPs-g-C_3N_4	0.005–100	0.85	3
ECL/MIL-101(Al):Ru-PEI-Au	0.005–100	0.18	4
Electrochemistry/AuNPs-TSA	0.05–100	0.10	5
Fluorescence/CdTeQDs	0.1–10	0.25	6
Photoelectrochemical immunosensor/NCQDs	0.001–100	0.42	7
ECL/MnO_2NFs/PDDA-Ag/ZnSQDs	0.0001–100	0.033	This work

References

1 Y. Hu, Z. Xue, H. He, R. Ai, X. Liu and X. Lu, Biosens. Bioelectron., 2013, **47**, 45-49.

2 H. Lv, R. Zhang, S. Cong, J. Guo, M. Shao, W. Liu, L. Zhang and X. Lu, Anal. Chem., 2022, **94**, 4538-4546.

3 P. Xu, Y. Zhang, X. Li, X. Ren, D. Fan, H. Wang, Q. Wei and H. Ju, Sensor. Actuat. B-Chem., 2021, **329**, 129101.

4 C. Wang, N. Zhang, D. Wei, R. Feng, D. Fan, L. Hu, Q. Wei and H. Ju, Biosens. Bioelectron., 2019, **142**, 111521.

5 P. Liu, C. Li, R. Zhang, Q. Tang, J. Wei, Y. Lu and P. Shen, Biosens. Bioelectron., 2019, **126**, 543-550.

6 Y. Zhou, X. Shao, Y. Han and H. Zhang, Anal. Methods-UK, 2018, **10**, 1015-1022.

7 X. Liu, C. Bao, X. Shao, Y. Zhang, N. Zhang, X. Sun, D. Fan, Q. Wei and H. Ju, New. J. Chem., 2020, **44**, 2452-2458.